# A New SEPIC Inverter: Small Signal Modeling

Shweta Hegde, *Student Member, IEEE,* Afshin Izadian, *Senior Member, IEEE*
Energy Systems and Power Electronics Laboratory
Purdue School of Engineering and Technology, Indianapolis
aizadian@iupui.edu

***Abstract*— This paper presents a new inverter technology that is designed based on SEPIC converter. Small signal model and transfer functions of the inverter are obtained. The system demonstrates the existence of a non-minimum phase zero in positive peak and shift of that zero to left half plane to make the negative peak transfer function a minimum phase behavior. Simulations demonstrate that at various circuit parameter values, as the duty cycle increased in boost mode of operation, the transfer function zeros migrated towards the origin. Increasing the inductance values resulted in similar behavior. However, increasing the capacitance values resulted in a reduction in real part of the complex poles and zeros.**

## I. Introduction

The SEPIC inverter shown in Figure 1 is a fourth order nonlinear system. The nonlinearity is originated from their inherent switching behaviour, which makes the stability analysis, designing and evaluating controllers difficult. The most common, systematic and successful approach to these tasks is linearization. Stability of the linearized model or small signal model indicates the system is stable when operating under nominal operating conditions for small perturbations [1]. System is linearized in a region around the operating point where the system response is assumed to be linear [2].

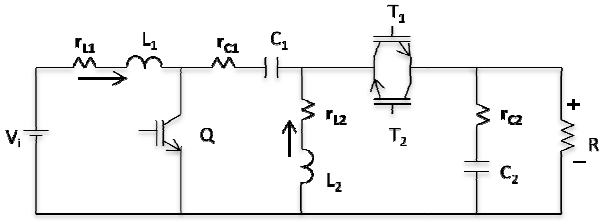


Fig. 1. Schematic Diagram of the New SEPIC Inverter

The state-space averaging (SSA) technique is applied to find small-signal linear dynamic model of the converter and its various transfer functions. As opposed to the PWM-switch model and averaged switch model, the SSA is a matrix-based approach in that all modeling steps in the SSA are performed systematically via matrices. Hence, mathematical software such as MATLAB can readily be used to aid the modeling process [10].

The transfer function is found to have two pairs of complex poles on the left half plane while the positions of the zeros are observed with variation in component values. The study of movement of poles and zeros of the system allows us to determine if the system is stable and has minimal or non-minimal phase. Knowledge about the system being a minimal phase or non-minimal phase system helps us to decide the type of control required for the system [3]-[7]. Simple techniques like Model Reference Adaptive Control can be used for minimal phase systems while for non-minimal phase system, control techniques like backstepping, sliding mode, self-tuning controllers may be required [8].

## II. Small Signal Derivation

Small signal analysis is a mathematical method for studying the dynamic response of the system when perturbed by a small disturbance. It is a technique of analyzing the behavior of a non-linear system with linear equations. The system is linearized around the DC operating point. The assumption made here is that the perturbation in the signal is small and is insufficient to cause any change in the operating point of the system. The small signal model can be derived by assuming each signal to be sum of a constant DC value and small AC perturbation. The DC quantities present in the model are considered to be constant and cancel of on either side of the voltage equations for inductors and current equations for capacitors, thus can be eliminated. In addition, the second order non-linear terms are eliminated as they are assumed to be negligible when compared to the first order AC terms.

Consider a switching circuit containing one switch such that the circuit switches between two different states in one switching period. There are two circuit states when the switch is operated. One state is when the switch is closed for duration of dT where d is the duty cycle and T is the switching time period. The other state is when the switch is open for duration of (1-d)T.

Consider the state space model of the circuit with index 1 when switch is closed as :$\begin{cases}\dot{x}(t) = A_1x(t) + B_1u(t) \\ y = C_1x(t) + E_1u(t)\end{cases}$ and with index 2 when the switch is open as: $\begin{cases}\dot{x}(t) = A_2x(t) + B_2u(t) \\ y = C_2x(t) + E_2u(t)\end{cases}$. The operation of the circuit averaged over one switching cycle

can be obtained as:

$$\begin{cases} \dot{x}(t) = A_{avg}\langle x(t)\rangle + B_{avg}\langle u(t)\rangle \\ y = C_{avg}\langle x(t)\rangle + E_{avg}\langle u(t)\rangle \end{cases} \quad (1)$$

where in

$A_{avg} = dA_1 + (1-d)A_2$, $B_{avg} = dB_1 + (1-d)B_2$

$C_{avg} = dC_1 + (1-d)C_2$, $E_{avg} = dE_1 + (1-d)E_2$

The terms in the brackets $\langle \ \rangle$ are the average values. The equation (1) is a nonlinear continuous time equation and it can be linearized by small signal perturbation. Each signal is replaced by a sum of two terms a fixed DC quantity and a small ac variation. The assumption made is that the perturbation is very small compared to the DC values. This perturbation yields the steady state and linear small signal state space equations as:

$$\begin{cases} \dot{X} = AX + BU = 0 \\ Y = CX + EU \end{cases}, \quad (2)$$

and

$$\begin{cases} \dot{\hat{x}} = A\hat{x}(t) + B\hat{u}(t) + B_d\hat{d}(t) \\ \hat{y} = C\hat{x}(t) + E\hat{u}(t) + E_d\hat{d}(t) \end{cases}, \quad (3)$$

where

$A = DA_1 + (1-D)A_2$

$B = DB_1 + (1-D)B_2$

$C = DC_1 + (1-D)C_2$

$E = DE_1 + (1-D)E_2$

$B_d = (A_1 - A_2)X + (B_1 - B_2)U$

$E_d = (C_1 - C_2)X + (E_1 - E_2)U.$

The steady state solution of the inverter can be found by solving (2) as:

$$\begin{cases} X = -A^{-1}BU \\ Y = (-CA^{-1}B + E)U \end{cases} \quad (4)$$

The small signal transfer function of the inverter can be obtained by applying Laplace transform to (3). In matrix form, we have

$$\begin{cases} \hat{x}(s) = [(sI-A)^{-1}B \quad (sI-A)^{-1}B_d]\begin{bmatrix}\hat{u}(s)\\ \hat{d}(s)\end{bmatrix} \\ \hat{y}(s) = [C(sI-A)^{-1}B + E \quad C(sI-A)^{-1}B_d + E_d]\begin{bmatrix}\hat{u}(s)\\ \hat{d}(s)\end{bmatrix} \end{cases} \quad (5)$$

The input variable $\hat{u}$ contains only the input voltage.

## III. SEPIC INVERTER

The SEPIC inverter operates in four different modes. The voltage equations around loops and current equations at nodes, which govern every mode of operation, can be written using KVL and KCL respectively.

The system is considered to have two inputs namely: input voltage $V_g$ and duty cycle d. The output of the system is the voltage across the load, $V_0$. To derive the small signal model, each signal is assumed to be the sum of a fixed DC value and a small time varying perturbation. The input voltage becomes $V_g + \hat{v}_g(t)$ and the duty cycle becomes $D + \hat{d}(t)$. The output voltage becomes $V_0 + \hat{v}_0(t)$ and the states become $X + \hat{x}(t)$ where $V_g$, $D$, $V_0$ and $X$ are the steady state operating point variables and the variables expressed with ^ are the small signal perturbations.

### A. Positive Cycle

The averaged state space representation of the system when operating to produce positive half cycle of output is

$$\begin{cases} \dot{x} = A^+_{avg}x + B^+_{avg}u + B^+_d d \\ V_o = C^+_{avg}x + E^+_d d \end{cases} \quad (6)$$

The positive peak averaged model parameters can be obtained as:

$$A^+_{avg} = \begin{bmatrix} \frac{1}{L_1}\left(-r_{L1} + (D-1)\left(rc1 + \frac{Rr_{C2}}{R+r_{C2}}\right)\right) & \frac{(D-1)Rr_{C2}}{L_1(R+r_{C2})} & \frac{D-1}{L_1} & \frac{(D-1)R}{L_1(R+r_{C2})} \\ \frac{(D-1)Rr_{C2}}{L_2(R+r_{C2})} & \frac{(D-1)Rr_{C2} - (R+r_{C2})(Dr_{C1}+r_{L2})}{L_2(R+r_{C2})} & \frac{D}{L_2} & \frac{(D-1)R}{L_2(R+r_{C2})} \\ \frac{1-D}{C_1} & -\frac{D}{C_1} & 0 & 0 \\ \frac{(1-D)R}{C_2(R+r_{C2})} & \frac{(1-D)R}{C_2(R+r_{C2})} & 0 & -\frac{1}{C_2(R+r_{C2})} \end{bmatrix}$$

$$B^+_{avg} = \begin{bmatrix}\frac{1}{L_1} & 0 & 0 & 0\end{bmatrix}^T, \quad C^+_{avg} = \begin{bmatrix}\frac{(1-D)Rr_{C2}}{(R+r_{C2})} & \frac{(1-D)Rr_{C2}}{(R+r_{C2})} & 0 & \frac{R}{R+r_{C2}}\end{bmatrix}$$

$$B^+_d = [B^+_{d11}\ B^+_{d21}\ B^+_{d31}\ B^+_{d41}]^T, \quad E^+_d = [E^+_{d11}]$$

Upon application of Laplace transform, equation (6) is transformed as shown in (7)

The small signal model for the system operating to produce positive cycle of output can be obtained from (7)

$$\begin{cases} sL_1\hat{\imath}_{L1}(s) = \hat{v}_g(s) - \hat{\imath}_{L1}(s)r_{L1} - D'\left(\hat{\imath}_{L1}(s)r_{C1} - \hat{v}_{C1}(s) - \hat{v}_0(s)\right) + \hat{d}(s)(I_{L1}r_{C1} + V_{C1} + V_0) \\ sC_1\hat{v}_{C1}(s) = D'\hat{\imath}_{L1}(s) + D\hat{\imath}_{L2}(s) + \hat{d}(s)(I_{L2} - I_{L1}) \\ sL_2\hat{\imath}_{L2}(s) = D(\hat{v}_{C1}(s) - \hat{\imath}_{L2}(s)r_{C1}) + D'\hat{v}_0(s) + \hat{d}(s)(V_{C1} - I_{L2}r_{C1} - V_0) - \hat{\imath}_{L2}(s)r_{L2} \\ sC_2\hat{v}_{C2}(s) = D'(\hat{\imath}_{L1}(s) + \hat{\imath}_{L2}(s)) - \hat{d}(s)(I_{L1} + I_{L2}) - \frac{\hat{v}_0(s)}{R} \\ \hat{v}_0(s) = \frac{Rr_{C2}}{R+r_{C2}}\left(D'\hat{\imath}_{L1}(s) + D'\hat{\imath}_{L2}(s) - \hat{d}(s)I_{L1} - \hat{d}(s)I_{L2}\right) + \frac{R}{R+r_{C2}}\hat{v}_{C2}(s) \end{cases} \quad (7)$$

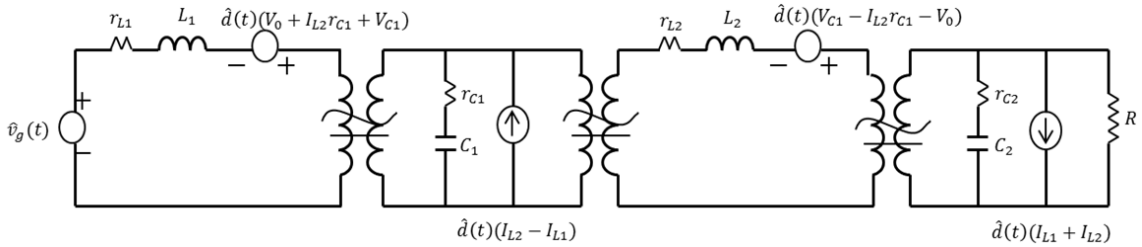


Fig. 2. Schematic diagram of Small Signal Model of the SEPIC Inverter when operating to produce positive cycle of output

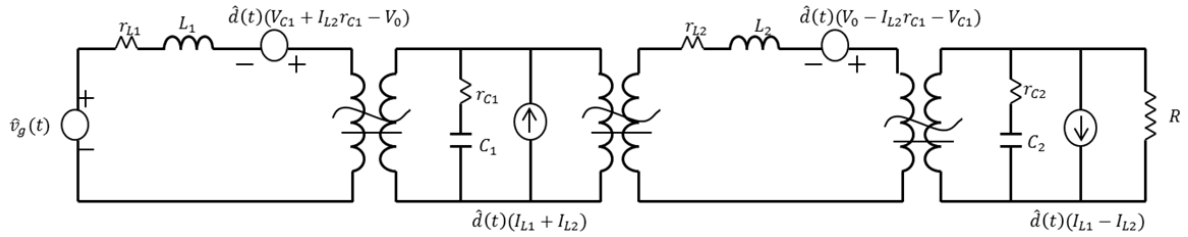


Fig. 3. Schematic diagram of Small Signal Model of the SEPIC Inverter when operating to produce negative cycle of output

*B. Negative Peak Voltage Generation*

The averaged state space representation of the system when operating to produce negative half cycle of output is

$$\begin{cases} \dot{x} = A_{avg}^{-}x + B_{avg}^{-}u + B_{\hat{d}}^{-}d \\ V_o = C_{avg}^{-}x + E_{\hat{d}}^{-}d \end{cases} \quad (8)$$

The negative peak averaged model parameters can be obtained as

$$A_{avg}^{-} = \begin{bmatrix} \frac{1}{L_1}\left(-r_{L1}+(D-1)\left(r_{C1}+\frac{Rr_{C2}}{R+r_{C2}}\right)\right) & \frac{(1-D)Rr_{C2}}{L_1(R+r_{C2})} & \frac{D-1}{L_1} & \frac{(1-D)R}{L_1(R+r_{C2})} \\ \frac{(1-D)Rr_{C2}}{L_2 2(R+r_{C2})} & -\frac{(Dr_{C1}+r_{L2})}{L_2}+\frac{(D-1)Rr_{C2}}{L_2(R+r_{C2})} & \frac{D}{L_2} & \frac{(D-1)R}{L_2(R+r_{C2})} \\ \frac{1-D}{C_1} & \frac{D}{C_1} & 0 & 0 \\ \frac{(D-1)R}{C_2(R+r_{C2})} & \frac{(1-D)R}{C_2(R+r_{C2})} & 0 & -\frac{1}{C_2(R+r_{C2})} \end{bmatrix}$$

$$B_{avg}^{-} = \left[\frac{1}{L_1}\ 0\ 0\ 0\right]^T, C_{avg}^{-} = \left[\frac{(D-1)Rrc}{C_2(R+rc2)}\ \ \frac{(1-D)Rrc2}{C_2(R+rc2)}\ 0\ \ \frac{R}{R+rc2}\right]$$

$$B_{\hat{d}}^{-} = [B_{\hat{d}11}^{-}\ B_{\hat{d}21}^{-}\ B_{\hat{d}31}^{-}\ B_{\hat{d}41}^{-}]^T, \quad E_{\hat{d}}^{-} = [E_{\hat{d}11}^{-}]$$

Upon application of Laplace transform, equation (8) is transformed as shown in (9).

$$\begin{cases} sL_1\hat{\imath}_{L1}(s) = \hat{v}_g(s) - \hat{\imath}_{L1}(s)r_{L1} - D'(\hat{\imath}_{L1}(s)r_{C1} - \hat{v}_{C1}(s) + \hat{v}_0(s)) + \hat{d}(s)(I_{L1}r_{C1} + V_{C1} - V_0) \\ sC_1\hat{v}_{C1}(s) = D'\hat{\imath}_{L1}(s) - D\hat{\imath}_{L2}(s) - \hat{d}(s)(I_{L1} + I_{L2}) \\ sL_2\hat{\imath}_{L2}(s) = -D(\hat{v}_{C1}(s) - \hat{\imath}_{L2}(s)r_{C1}) - D'\hat{v}_0(s) + \hat{d}(s)(V_0 - I_{L2}r_{C1} - V_{C1}) - \hat{\imath}_{L2}(s)r_{L2} \\ sC_2\hat{v}_{C2}(s) = D'(\hat{\imath}_{L2}(s) - \hat{\imath}_{L1}(s)) + \hat{d}(s)(I_{L1} - I_{L2}) - \frac{\hat{v}_0(s)}{R} \\ \hat{v}_0(s) = \frac{Rr_{C2}}{R+r_{C2}}\left(-D'\hat{\imath}_{L1}(s) + D'\hat{\imath}_{L2}(s) + \hat{d}(s)I_{L1} - \hat{d}(s)I_{L2}\right) + \frac{R}{R+r_{C2}}\hat{v}_{C2}(s) \end{cases} \quad (9)$$

*C. Steady State Equations*

In Mode I, the switch Q is on and $T_1$ is off for duty cycle D. In Mode II, the switch is off and $T_1$ is on for period of 1-D. The averaged state space model of the system for positive cycle of output voltage is given as:

*1) Positive Half-Cycle:* Given the averaged matrices in (6), the steady state equations of this inverter are obtained from (2) as:

$$\begin{bmatrix} I_{L1} \\ I_{L2} \\ V_{C1} \\ V_{C2} \end{bmatrix} = \begin{bmatrix} \frac{D}{D'\left(\frac{D}{D'}r_{L1}+r_{C1}+\frac{Rr_{C2}}{D(R+r_{C2})}+\frac{D'R^2}{D(R+r_{C2})}+\frac{D'}{D}r_{L2}\right)} \\ \frac{1}{\frac{D}{D'}r_{L1}+r_{C1}+\frac{Rr_{C2}}{D(R+r_{C2})}+\frac{D'R^2}{D(R+r_{C2})}+\frac{D'}{D}r_{L2}} \\ \frac{r_{L2}+Dr_{C1}+\frac{Rr_{C2}}{R+r_{C2}}+\frac{D'R^2}{R+r_{C2}}}{D\left(\frac{D}{D'}r_{L1}+r_{C1}+\frac{Rr_{C2}}{D(R+r_{C2})}+\frac{D'R^2}{D(R+r_{C2})}+\frac{D'}{D}r_{L2}\right)} \\ \frac{R}{\frac{D}{D'}r_{L1}+r_{C1}+\frac{Rr_{C2}}{D(R+r_{C2})}+\frac{D'R^2}{D(R+r_{C2})}+\frac{D'}{D}r_{L2}} \end{bmatrix}[V_g] \quad (10)$$

$$V_0 = \left[\frac{\frac{Rr_{C2}}{R+r_{C2}}+\frac{D'R^2}{R+r_{C2}}}{D'\left(\frac{D}{D'}r_{L1}+r_{C1}+\frac{Rr_{C2}}{D(R+r_{C2})}+\frac{D'R^2}{D(R+r_{C2})}+\frac{D'}{D}r_{L2}\right)}\right][V_g]$$

*2) Negative Half-Cycle:* Given the averaged matrices in (8), the steady state equations of this inverter are obtained from (2) as:

$$\begin{bmatrix} I_{L1} \\ I_{L2} \\ V_{C1} \\ V_{C2} \end{bmatrix} = \begin{bmatrix} \frac{D}{D'\left(\frac{D}{D'}r_{L1}+r_{C1}+\frac{Rr_{C2}}{D(R+r_{C2})}+\frac{D'R^2}{D(R+r_{C2})}+\frac{D'}{D}r_{L2}\right)} \\ \frac{-1}{\frac{D}{D'}r_{L1}+r_{C1}+\frac{Rr_{C2}}{D(R+r_{C2})}+\frac{D'R^2}{D(R+r_{C2})}+\frac{D'}{D}r_{L2}} \\ \frac{r_{L2}+Dr_{C1}+\frac{Rr_{C2}}{R+r_{C2}}+\frac{D'R^2}{R+r_{C2}}}{D\left(\frac{D}{D'}r_{L1}+r_{C1}+\frac{Rr_{C2}}{D(R+r_{C2})}+\frac{D'R^2}{D(R+r_{C2})}+\frac{D'}{D}r_{L2}\right)} \\ \frac{-R}{\frac{D}{D'}r_{L1}+r_{C1}+\frac{Rr_{C2}}{D(R+r_{C2})}+\frac{D'R^2}{D(R+r_{C2})}+\frac{D'}{D}r_{L2}} \end{bmatrix}[V_g] \quad (11)$$

$$V_0 = \left[\frac{-\frac{Rr_{C2}}{R+r_{C2}}-\frac{D'R^2}{R+r_{C2}}}{D'\left(\frac{D}{D'}r_{L1}+r_{C1}+\frac{Rr_{C2}}{D(R+r_{C2})}+\frac{D'R^2}{D(R+r_{C2})}+\frac{D'}{D}r_{L2}\right)}\right][V_g]$$

## IV. Inverter Transfer Functions

State space averaging techniques have been employed to derive the transfer functions and small signal model of the inverter after mathematical analysis.

The AC output voltage $\hat{v}_0(t)$ can be expressed as the superposition of the terms arising from the two inputs

$$\hat{v}_0(s) = G_d^{v_0}(s)\hat{d}(s) + G_{v_g}^{v_0}(s)\hat{v}_g(s) \quad . \quad (12)$$

The first term in (12) represents the control to output transfer function while the second term represents the line to output transfer function. The transfer functions $G_d^{v_0}(s)$ and $G_{v_g}^{v_0}(s)$ can be defined as:

$$G_d^{v_0}(s) = \left.\frac{\hat{v}_0(s)}{\hat{d}(s)}\right|_{\hat{v}_g(s)=0} \quad and \quad G_{v_g}^{v_0}(s) = \left.\frac{\hat{v}_0(s)}{\hat{v}_g(s)}\right|_{\hat{d}(s)=0}$$

From (5), the various transfer functions can be determined as follows:

The control to output and line voltage to output transfer functions can be determined using the equations shown in (13)

$$\begin{cases} G_d^{v_0}(s) = C(sI-A)^{-1}B_d + E_d \\ G_{v_g}^{v_0}(s) = C(sI-A)^{-1}B + E \end{cases} \quad . \quad (13)$$

The transfer functions for the control to inductor currents, control to capacitor voltages can be derived from (5) as follows:

$$\begin{cases} G_d^{i_{L1}}(s) = [(sI - A)^{-1}B_d]_{11} \\ G_d^{i_{L2}}(s) = [(sI - A)^{-1}B_d]_{21} \\ G_d^{v_{c1}}(s) = [(sI - A)^{-1}B_d]_{31} \\ G_d^{v_{c2}}(s) = [(sI - A)^{-1}B_d]_{41} \end{cases} \quad (14)$$

The transfer functions of line voltage to inductor currents and capacitor voltages are determined from (5) as:

$$\begin{cases} G_{v_g}^{i_{L1}}(s) = [(sI - A)^{-1}B]_{11} \\ G_{v_g}^{i_{L2}}(s) = [(sI - A)^{-1}B]_{21} \\ G_{v_g}^{v_{c1}}(s) = [(sI - A)^{-1}B]_{31} \\ G_{v_g}^{v_{c2}}(s) = [(sI - A)^{-1}B]_{41} \end{cases} \quad (15)$$

The control to output transfer function is studied to determine if the system has any right half plane zeros. The presence of right half zeros implies system is non-minimal phase. Control of such systems is complicated compared to minimal phase systems. The values of the circuit components may be varied to check if the zeros can be moved from the right half plane to the left half plane.

Various transfer functions of the inverter are derived in (13) - (15). The transfer functions of the control to inductor currents and capacitor voltages are given in (14). The transfer function for the line voltage to inductor currents and capacitor voltages are given in (15). However, only the control to output transfer function is analyzed.

*1) Positive Half Cycle:* The structure of the control to output transfer function is:

$$G_d^{v_0}(s) = \frac{N_{p4}s^4 + N_{p3}s^3 + N_{p2}s^2 + N_{p1}s + N_{p0}}{D_{p4}s^4 + D_{p3}s^3 + D_{p2}s^2 + D_{p1}s + D_{p0}} \quad (16)$$

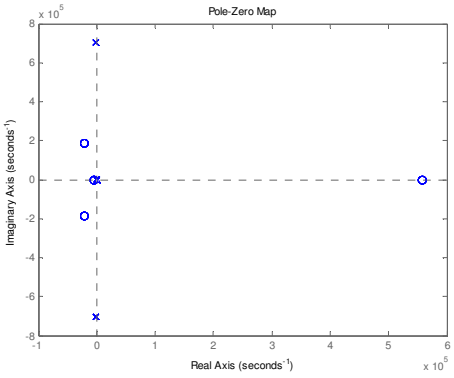


Fig. 4. Root-locus for variation in Capacitance

The system when operating to produce positive half cycle of output voltage has four zeros of which one is in the right half plane making the system non-minimal phase. All four poles of the system lie in the left half plane. It is important to study the movement of poles and zeros of the system in its entire operating range to keep satisfactory performance and stability [2]. The root-locus are plotted and studied when one parameter is varied at a time. The input inductor $L_1$, coupling capacitor $C_1$ and duty cycle D are varied separately while keeping all other parameters constant. The plots are analyzed to check the region in the operating range which would give satisfactory response.

From Figure 4, it can be seen that the position of poles and zeros do not change with any change in the value of $C_1$ from 1 µF to 50 µF.

From Figure 5, it can be seen that as the value of inductance $L_1$ is varied from 1 µH to 50 µH , the right half plane (RHP) zero moves towards the imaginary axis along the real axis but does not cross over to the left half plane (LHP). The poles of the system move towards the real axis and always remain in the LHP. The movement of poles of the system may increase the damping of the system to reduce the overshoot or undershoot but increases the settling time of the system.

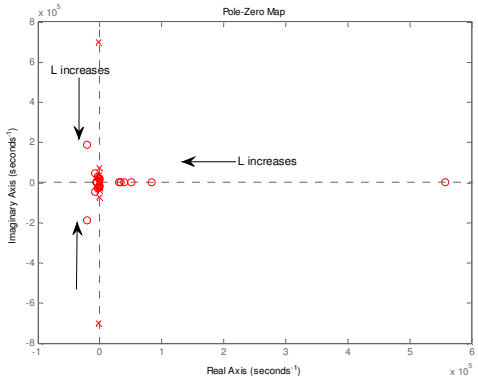


Fig. 5. Root-locus for variation in Inductance

From Figure 6, it can be seen that as the duty cycle of the system is varied over its entire range i.e. from 0.1 to 0.9 to check for buck and boost operation, the RHP zero moves closer to the LHP but never moves into this region. The system remains non-minimum phase for buck and boost operation. The LHP zero does not move for any change in duty cycle while the complex pair of LHP zeros move towards the origin but do not cross over to the RHP.

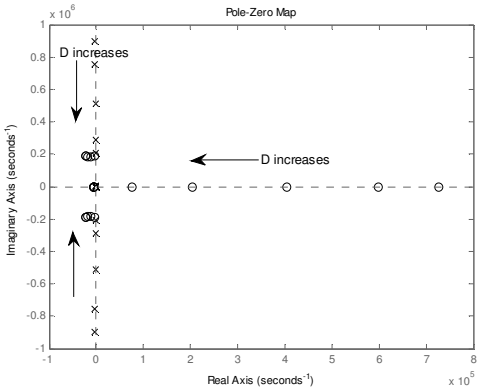


Fig. 6. Root-locus for variation in duty cycle

*2) Negative Half Cycle:* The structure of control to output transfer function is:

$$G_d^{v_0}(s) = \frac{N_{n4}s^4+N_{n3}s^3+N_{n2}s^2+N_{n1}s+N_{n0}}{D_{n4}s^4+D_{n3}s^3+D_{n2}s^2+D_{n1}s+D_{n0}}. \quad (17)$$

When the system is operating to produce negative cycle of output voltage, it has four poles all of which are in the LHP ensuring stable operations. The system has four zeros all in the LHP. The Root-locus has been plotted to study the movement of poles and zeros to determine a region of stable operation and satisfactory response. One parameter is varied at a time to check the movement of poles and zeros while other parameters are fixed. The parameters varied are inductance $L_1$, capacitance $C_1$ and duty cycle D.

From Figure 7, it can be seen that as the value of $C_1$ is varied from 1µF to 50 µF, all the zeros remain in the LHP and move towards the real axis as the capacitance is increased. The poles of the system also move towards the real axis with increase in capacitance and always remain in the LHP.

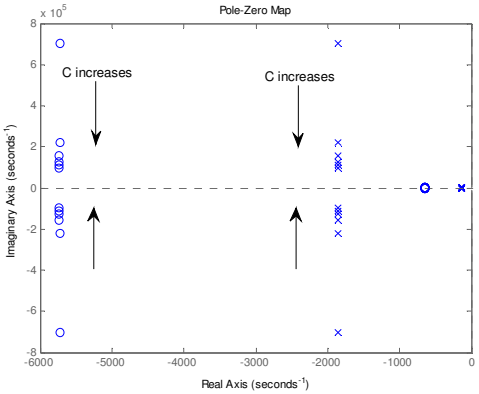


Fig. 7. Root-locus for variation in Capacitance

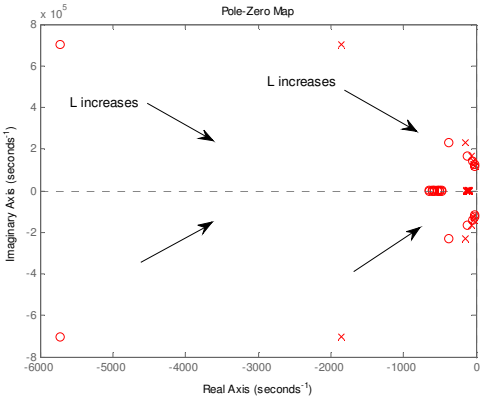


Fig. 8. Root-locus for variation in Inductance

From Figure 8, it can be seen that as the value of inductance $L_1$ is varied from 1 µH to 50 µH, the zeros continue to remain in the LHP. However, as the inductance is increased, the zeros move closer to the real axis and towards the RHP but do not cross over into the RHP. The poles of the system also move closer to the imaginary axis and lower towards the real axis as inductance is increased. However, the poles never move into the RHP.

From Figure 9, it can be seen that as the duty cycle D is increased, the zeros remain in the LHP for duty cycle up to 50% i.e. buck operation. However, when the duty is increased beyond 50% i.e. to give boost operation, one LHP zero moves in the RHP. Thus, the system operating to produce negative peak of magnitude greater than input voltage will behave like a non-minimal phase system. However, the poles always remain in the LHP and move closer to the origin.

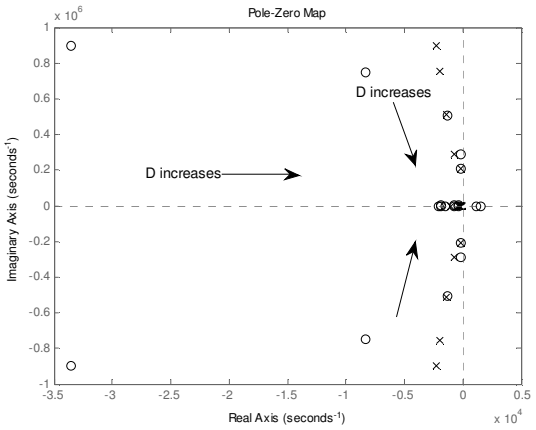


Fig. 9. Root-locus for variation in duty cycle

## V. CONCLUSIONS

The small signal model of the SEPIC inverter was developed using the state space averaging technique. The transfer functions of the inverter for the positive and negative cycle are derived and the control to output transfer function is analyzed using root locus. The root locus is studied for variation in component values to determine the movement of zeros and poles of the system. This helped us determine the operating region of the inverter which would give satisfactory response and stability. Analysis of control to output transfer function will also help us to determine which controller can be used to stabilize the system. The transfer function of SEPIC has two pairs of complex poles which causes two resonant peaks. The system has four zeros which may lie in LHP or RHP depending on the parameter values and whether the inverter is operating in buck or boost mode.

## REFERENCES

[1] Bauer, P.; van Duijsen, P.J., "Large signal and small signal modeling techniques for AC-AC power converters," *Power Conversion Conference, 1993. Yokohama 1993., Conference Record of the* , vol., no., pp.520,525, 19-21 April 1993.

[2] Cantillo, A.; De Nardo, A.; Femia, N.; Zamboni, W., "Stability Issues in Peak-Current-Controlled SEPIC," *Power Electronics, IEEE Transactions on* , vol.26, no.2, pp.551,562, Feb. 2011.

[3] Li, Yuan; Peng, Fang Z., "AC small signal modeling, analysis and control of quasi-Z-Source Converter," *Power Electronics and Motion Control Conference (IPEMC), 2012 7th International* , vol.3, no., pp.1848,1854, 2-5 June 2012

[4] Thang, T. V.; Thao, N. M.; Do-Hyun Kim; Joung-Hu Park, "Analysis and design of a single-phase Flyback microinverter on CCM operation," *Power Electronics and Motion Control Conference (IPEMC), 2012 7th International* , vol.2, no., pp.1229,1234, 2-5 June 2012

[5] Jingbo Liu; Jiangang Hu; Longya Xu, "Dynamic Modeling and Analysis of Z Source Converter—Derivation of AC Small Signal Model and Design-Oriented Analysis," *Power Electronics, IEEE Transactions on* , vol.22, no.5, pp.1786,1796, Sept. 2007

[6] Kun Yu; Fang-Lin Luo; Miao Zhu, "Study of an improved Z-source inverter: Small signal analysis," *Industrial Electronics and Applications (ICIEA), 2010 the 5th IEEE Conference on* , vol., no., pp.2169,2174, 15-17 June 2010

[7] Loh, P.C.; Vilathgamuwa, D.M.; Gajanayake, C.J.; Lim, Y. R.; Teo, C.W., "Transient modeling and analysis of pulse-width modulated Z-source inverter," *Industry Applications Conference, 2005. Fourtieth IAS Annual Meeting. Conference Record of the 2005* , vol.4, no., pp.2782,2789 Vol. 4, 2-6 Oct. 2005

[8] P. Ioannou & B. Fidan, *Adaptive Control Tutorial*, SIAM, Philadelpia, PA, 2006.

[9] R. W. Erickson and D. Maksimovic, *Fundamentals of Power Electronics*, $2^{nd}$ edition, Kluwer Academic Publishers, 2001.

[10] Vuthchhay, E.; Bunlaksananusorn, C., "Modeling and control of a Zeta converter," *Power Electronics Conference (IPEC), 2010 International* , vol., no., pp.612,619, 21-24 June 2010.

[11] Veda Prakash, G.N.; Kazimierczuk, M.K., "Small-Signal Modeling of Open-Loop PWM Z-Source Converter by Circuit-Averaging Technique," *Power Electronics, IEEE Transactions on* , vol.28, no.3, pp.1286,1296, March 2013

[12] Lineykin, S.; Ben-Yaakov, S., "A unified SPICE compatible model for large and small signal envelope simulation of linear circuits excited by modulated signals," *Power Electronics Specialist Conference, 2003. PESC '03. 2003 IEEE 34th Annual* , vol.3, no., pp.1205,1209 vol.3, 15-19 June 2003

[13] Ma Hua-sheng; Zhang Bo; Zheng Jian-chao, "Three-Phase PWM AC-AC Buck Converter Small-signal Modeling, Dynamic Analysis and Control System Design," *Power Electronics Specialists Conference, 2006. PESC '06. 37th IEEE* , vol., no., pp.1,5, 18-22 June 2006

[14] Zhang, X.; Spencer, J.; Guerrero, J., "Small-Signal Modeling of Digitally Controlled Grid-Connected Inverters with LCL filters," *Industrial Electronics, IEEE Transactions on* , vol.PP, no.99, pp.1,1, 0

[15] Kanaan, H.-Y.; Marquis, A.; Al-Haddad, K., "Small-signal modeling and linear control of a dual boost power factor correction circuit," *Power Electronics Specialists Conference, 2004. PESC 04. 2004 IEEE 35th Annual* , vol.4, no., pp.3127,3133 Vol.4, 2004

[16] Tajuddin, M. F N; Rahim, N.A., "Small-signal AC modeling technique of Buck converter with DSP based Proportional-Integral-Derivative (PID) controller," *Industrial Electronics & Applications, 2009. ISIEA 2009. IEEE Symposium on* , vol.2, no., pp.904,909, 4-6 Oct. 2009

[17] Michal, V., "Modulated-Ramp PWM Generator for Linear Control of the Boost Converter's Power Stage," *Power Electronics, IEEE Transactions on* , vol.27, no.6, pp.2958,2965, June 2012

[18] Fernandez, A.; Sebastian, J.; Hernando, M.M.; Lamar, D.G.; de Azpeitia, M.; Rodriguez, M., "Modeling of an AC-to-DC Converter With a Single-Stage Power Factor Corrector," *Industrial Electronics, IEEE Transactions on* , vol.55, no.8, pp.3064,3076, Aug. 2008

[19] Xiaoyan Wang; Jih-Sheng Lai, "Small-signal modeling and control for PWM control of switched reluctance motor drives," *Power Electronics Specialists Conference, 2002. pesc 02. 2002 IEEE 33rd Annual* , vol.2, no., pp.546,551 vol.2, 2002

[20] Seroji, M.N.; Forsyth, A.J., "Small-Signal Model of a High-Power-Factor, Three-Phase AC-DC Converter with High-Frequency Resonant Current Injection," *Power Electronics and Drives Systems, 2005. PEDS 2005. International Conference on* , vol.1, no., pp.462,467, 0-0 0

[21] Karimi, Y.; Nasirian, V.R.; Ahmadian, M.; Yaghoobi, J.; Zolghadri, M.-R.; Ferdowsi, M., "Small-signal model development for a Cúk converter while operating in DCVM for both DC and AC input voltages," *Energy Conversion Congress and Exposition (ECCE), 2010 IEEE* , vol., no., pp.2613,2619, 12-16 Sept. 2010

[22] Rahman, A.; Bhat, A. K S, "Small-signal analysis of a soft-switching, new gating scheme controlled single-stage bridge AC-to-DC converter," *Power Electronics Specialists Conference, 2004. PESC 04. 2004 IEEE 35th Annual* , vol.1, no., pp.196,202 Vol.1, 20-25 June 2004

[23] Ng, S. W.; Wong, S.C., "Small signal simulation of switching converters," *Circuits and Systems I: Fundamental Theory and Applications, IEEE Transactions on* , vol.46, no.6, pp.731,739, Jun 1999

[24] Alsseid, A.M.; Jovcic, D.; Starkey, A., "Small signal modelling and stability analysis of multiterminal VSC-HVDC," *Power Electronics and Applications (EPE 2011), Proceedings of the 2011-14th European Conference on* , vol., no., pp.1,10, Aug. 30 2011-Sept. 1 2011

[25] Byungcho Choi; Sung-Soo Hong; Hyokil Park, "Modeling and small-signal analysis of controlled on-time boost power-factor-correction circuit," *Industrial Electronics, IEEE Transactions on* , vol.48, no.1, pp.136,142, Feb 2001

[26] Niculescu, E.; Iancu, E.-P., "Modeling and analysis of the DC/DC fourth-order PWM converters," *Computers in Power Electronics, 2000. COMPEL 2000. The 7th Workshop on* , vol., no., pp.83,88, 2000

[27] Ngo, K. D T, "Low Frequency Characterization of PWM Converters," *Power Electronics, IEEE Transactions on* , vol.PE-1, no.4, pp.223,230, Oct. 1986

[28] Jingbo Liu; Jiangang Hu; Longya Xu, "Dynamic Modeling and Analysis of Z Source Converter—Derivation of AC Small Signal Model and Design-Oriented Analysis," *Power Electronics, IEEE Transactions on* , vol.22, no.5, pp.1786,1796, Sept. 2007

[29] Adda, R.; Mishra, S.; Joshi, A., "Analysis and PWM Control of Switched Boost Inverter," *Industrial Electronics, IEEE Transactions on* , vol.PP, no.99, pp.1,1, 0